











**Spontaneous creation and annihilation dynamics of magnetic skyrmions at elevated temperature**

Junlin Wang <sup>1,2</sup>, Mara Strungaru,<sup>3</sup> Sergiu Ruta,<sup>3</sup> Andrea Meo <sup>3</sup>, Yifan Zhou <sup>4</sup>, András Deák <sup>5</sup>, László Szunyogh <sup>5,6</sup>, Paul-Iulian Gavriloaea <sup>3</sup>, Roberto Moreno <sup>7</sup>, Oksana Chubykalo-Fesenko <sup>8</sup>, Jing Wu,<sup>3,2</sup> Yongbing Xu,<sup>1,2,\*</sup> Richard F. L. Evans <sup>3</sup> and Roy W. Chantrell <sup>3,†</sup>

<sup>1</sup>*Spintronics and Nanodevice laboratory, Department of Electronic Engineering, University of York, York YO10 5DD, United Kingdom*

<sup>2</sup>*York-Nanjing International Center of Spintronics (YNICS), Nanjing University, Nanjing 210093, China*

<sup>3</sup>*Department of Physics, University of York, York YO10 5DD, United Kingdom*

<sup>4</sup>*NanoSpin, Department of Applied Physics, Aalto University School of Science, P.O. Box 15100, FI-00076 Aalto, Finland*

<sup>5</sup>*Department of Theoretical Physics, Budapest University of Technology and Economics, Budapest 1111, Hungary*

<sup>6</sup>*MTA-BME Condensed Matter Research Group, Budapest University of Technology and Economics, Budapest 1111, Hungary*

<sup>7</sup>*Earth and Planetary Science, School of Geosciences, University of Edinburgh, Edinburgh EH9 3FE, United Kingdom*

<sup>8</sup>*Instituto de Ciencia de Materiales de Madrid, CSIC, Cantoblanco, 28049 Madrid, Spain*



(Received 2 March 2021; revised 21 June 2021; accepted 15 July 2021; published 13 August 2021)

Skyrmions are topologically protected nanoscale magnetic structures with a wide range of potential applications. Here we determine the life cycle of skyrmions from their creation to their intrinsic dynamics and thermal stability to their eventual thermodynamic demise. Using atomistic simulations of Ir/Co/Pt, parameterized from *ab initio* calculations, we demonstrate the thermal phase transition to a skyrmion state under application of a perpendicular magnetic field. The created skyrmions exhibit Brownian particlelike dynamics driven by the underlying thermal spin fluctuations. At an elevated temperature window well below the Curie temperature, the skyrmions are metastable and can collapse to a uniform magnetic state. With application of an external magnetic field, the intrinsic local thermal spin fluctuations at this elevated temperature window are sufficiently large to allow the spontaneous formation of new skyrmions in thermodynamic equilibrium analogous to a spontaneous skyrmion gas. Such a system could be used to implement a skyrmion-based true random number generator.

DOI: [10.1103/PhysRevB.104.054420](https://doi.org/10.1103/PhysRevB.104.054420)

**I. INTRODUCTION**

The magnetic skyrmion is a topological nontrivial magnetization configuration, shown to be found in magnetic materials which exhibit antisymmetric exchange, also known as the Dzyaloshinskii-Moriya interaction (DMI) [1–5]. The DMI relies on spin-orbit coupling, which usually is provided by the heavy metal layer in the system [6]. Skyrmions can be used as building blocks in the development of next-generation logic and data storage devices. In comparison with domain walls, skyrmions represent better candidates for potential applications due to the lower critical current threshold ( $10^6$  A/m<sup>2</sup>) to move them [7–9]. In nanoscale devices, skyrmion motion can be driven via spin polarized currents, spin waves, and temperature gradients [10–13]. During the displacement of magnetic skyrmions driven by a current or gradient in the nanoscale device, the Magnus force on the skyrmion causes it to move toward the edge, a phenomenon known as the skyrmion Hall effect [14]. Magnetic skyrmion-based devices are suggested for future data storage device applications. However, thermal effects arising from the environment or spin-polarized currents affect the practical application of magnetic skyrmion-based spintronic devices [15–18].

Thermal activation has usually been considered detrimental to magnetic skyrmions due to its potential to bypass their topological protection, thus being able to irreversibly deform or switch the chiral structures. Previous results have shown that skyrmions can be created by Joule heating and temperature gradients present in the device [17,19], but there is little published information on the behavior of magnetic skyrmions under strong thermal effects. The study of thermal effects in skyrmions can provide guidelines for room-temperature skyrmion-based devices [20–23] and give further insight on the generation mechanisms of skyrmions via temperature pulses that have been observed both by calculations and experiments [19,24,25]. Furthermore, the thermally induced skyrmion creation/annihilation and skyrmion dynamics show their potential as true random seed generators and provide insight on skyrmion transport under elevated temperature conditions [26–30]. It is necessary to develop suitable models to study skyrmion dynamics at elevated temperatures. At the moment, there are models based mainly on micromagnetic simulations [27,28], however, atomistic simulation with the full range of exchange interactions from *ab initio* calculations [30–32] is an important model to investigate skyrmion behavior at high temperatures. Atomistic simulations can model the time evolution of the spin configurations of skyrmion-based devices at elevated temperature and explain how the thermal effect affects device performance.

In this paper, we use atomistic spin dynamics simulations with *ab initio* parametrization to investigate skyrmion dynam-

\*yongbing.xu@york.ac.uk

†roy.chantrell@york.ac.uk

ics at elevated temperatures well below the Curie temperature ( $T_c$ ). The elevated temperature in this paper is taken from 300 K ( $0.461 T_c$ ) to 500 K ( $0.769 T_c$ ). The results in this paper present a time-resolution dynamics of skyrmion creation and annihilation in magnetic chiral thin films under strong thermal effect. The simulation results reveal thermally induced phase transitions between the skyrmion, stripe domain, and ferromagnetic states. We explore the behavior of the ferromagnetic and stripe domain states under different thermal processes as well as the required conditions for skyrmion creation and annihilation. Our results show that even at temperatures below the Curie temperature, it is possible to spontaneously generate a skyrmion in the thin film through a purely intrinsic thermal effect, circumventing their assumed feature of being topologically protected structures.

## II. MODELING AND SIMULATION

The simulations have been performed using the atomistic spin dynamics software package VAMPIRE 5.0 [33]. The model is based on the parameters from *ab initio* calculations and includes the full range of exchange interactions of the FCC Ir/Co/Pt system. Self-consistent calculations were performed for a model multilayer of 3Co/3Ir/3Co/3Pt/3Co layers sandwiched from both sides by Pt(111) by using the screened Korringa-Kohn-Rostoker method [34,35]. The electronic structure was determined in the paramagnetic state in terms of the scalar-relativistic disordered local moment (DLM) approach [36], while the spin-cluster expansion technique as combined with the relativistic DLM technique [37] was employed to derive tensorial exchange interactions. The spin Hamiltonian  $H$  of the system is described by an extended Heisenberg spin model with the following form:

$$H = - \sum_{i < j} (\mathbf{S}_i \mathbf{J}_{ij} \mathbf{S}_j) - k_u \sum_i (\mathbf{S}_i \cdot \mathbf{e})^2 - \sum_i \mu_i (\mathbf{S}_i \cdot \mathbf{B}_{\text{app}}), \quad (1)$$

where  $\mathbf{S}_i$ ,  $\mathbf{S}_j$  are the normalized spin vectors on  $i$ ,  $j$  sites,  $J_{ij}$  is the exchange matrix calculated *ab initio*,  $k_u$  is the uniaxial magnetocrystalline anisotropy energy (MAE) constant per site,  $\mu_i$  is the atomic spin moment, and  $\mathbf{B}_{\text{app}}$  is the external field. The *ab initio* exchange matrix is defined below, where the off-diagonal parts of the matrix represent the DMI vector components,  $D_{ij}$ :

$$\mathbf{J}_{ij} = \begin{bmatrix} J_{xx} & J_{xy} & J_{xz} \\ J_{yx} & J_{yy} & J_{yz} \\ J_{zx} & J_{zy} & J_{zz} \end{bmatrix}_{ij} = \begin{bmatrix} J_{xx} & J_{xy}^S + D_z & J_{xz}^S - D_y \\ J_{xy}^S - D_z & J_{yy} & J_{yz}^S + D_x \\ J_{xz}^S + D_y & J_{yz}^S - D_x & J_{zz} \end{bmatrix}_{ij}. \quad (2)$$

The model considers finite temperature via the introduction of the stochastic field into the effective field in the atomistic Landau-Lifshitz-Gilbert equation [38]. Within this approach, the stochastic field is introduced as a white noise term, its properties being in agreement with the fluctuation-dissipation theorem and correctly leading to the Boltzmann equilibrium distribution [39–41]. The accuracy of the results is assured by a integration timestep of  $5 \times 10^{-16}$  s. In this paper, we

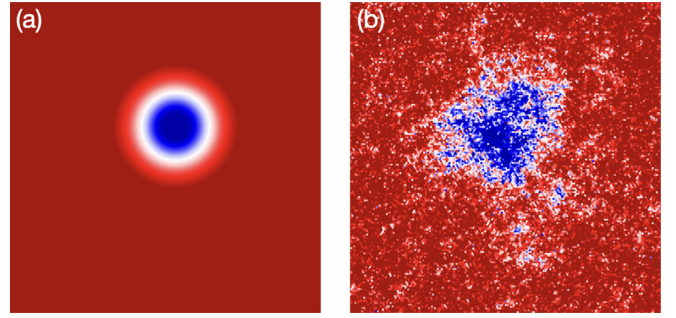


FIG. 1. Thin film spin configurations of an isolated skyrmion at different temperatures: (a) 0 K skyrmion ground state, (b) 300 K room-temperature skyrmion deformation. The color palette is determined by the  $M_z$  (red for +1, white for 0, and blue for -1).

explicitly include in our atomistic model only the three Cobalt layers between the Ir and Pt. The parameters for the atomistic spin model are given in the Supplemental Material [42]. The skyrmion number in this paper is calculated from the topological charge [32,43].

## III. RESULTS AND DISCUSSION

There are three magnetic phases in the Ir/Co/Pt multilayer system: the ferromagnetic phase, the stripe domain phase, and the skyrmion phase, which has also been found in other systems [2,44]. Skyrmion simulations at elevated temperatures also show the thermally induced phase transition between these three phases. The initial spin configurations are given in Fig. S3 in the Supplemental Material [42]. The system size is  $30 \text{ nm} \times 30 \text{ nm} \times 0.25 \text{ nm}$ , with periodic boundary conditions in the  $x$  and  $y$  directions. The ferromagnetic and the stripe domain configurations are obtained by relaxing the system at 0 K in zero applied field, while the skyrmion phase is obtained in a 1 T field relaxation process. When the temperature is higher than 100 K, the stripe domain will be generated by the thermal effect and the mean-magnetization length will drop to near 0, which means the ferromagnetic state is no longer the ground state of the system.

The ground-state skyrmion phase and the same structure visualized at an elevated temperature is shown in Fig. 1. The diameter of the skyrmion is around 5 nm at 0 K, while thermal noise leads to a significant distortion of the skyrmion structure, although the characteristic size is not significantly different.

We first consider the stripe domain phase under high temperature conditions (300 K to 500 K). The simulation time has been set to 10 ns, which is long enough to give a clear diagram of the phase transition in the system. The initial state for the spin configuration is given in Fig. S3(c). The stripe domain state can be stable without external field at 0 K. The 10 ns simulation of the stripe domain state for different temperatures is given in Fig. 2. Here thermal effects distort the shape of the stripe domains and we define a critical temperature at which the stripe domains undergo a phase transition. Below this threshold temperature, the spin texture diffuses due to the thermal fluctuations but its overall morphology is unchanged. Above the critical point, the system displays a thermally

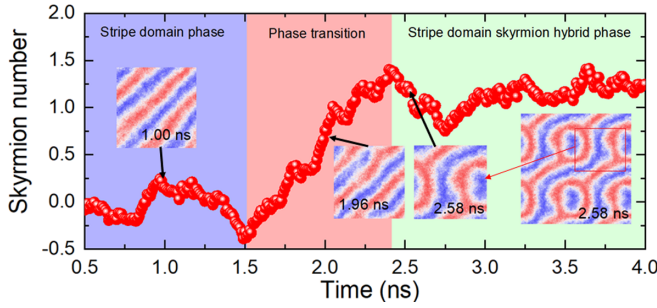


FIG. 2. The spin configuration of the stripe domain broken at 450 K. The system displays an initial stripe domain phase followed by a transition toward a hybrid stripe domain-skyrmion phase.

induced stripe-domain bending. This effect generates a hybrid magnetic configuration in which both skyrmions and stripe domains can be found. The result from Fig. 2 to Fig. 4 is averaged from ten spin configurations in the same time range to avoid large fluctuations from the strong thermal noise and give a better representation of the phase change.

Figure 2 further investigates this behavior, highlighting the time evolution of the striped texture at a temperature of 450 K. During the first 1.5 ns, it can be seen how the thermally induced diffusion process alters the magnetic configuration. Gradually moving our perspective in time, we find a bending

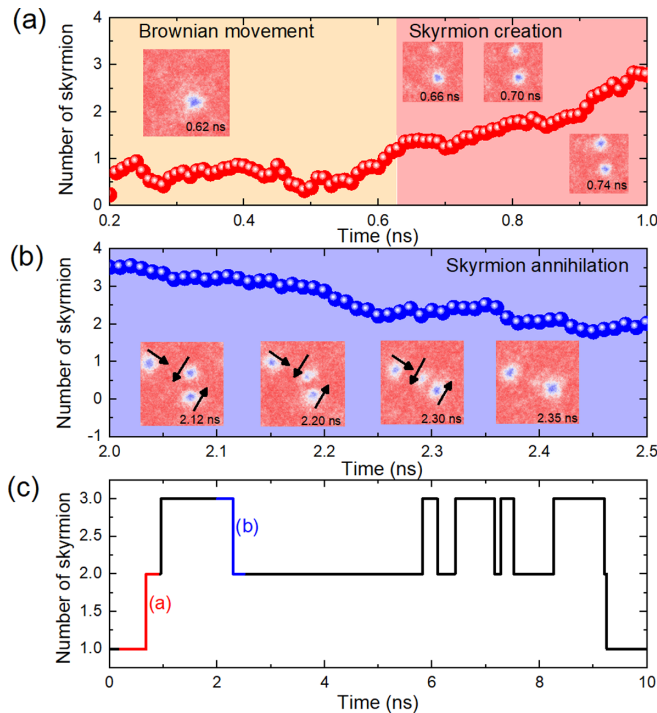


FIG. 3. (a) The spin configurations and skyrmion number during the skyrmion creation in the system. (b) The spin configurations and skyrmion number during skyrmion annihilation in the system. The spin configuration for skyrmion nucleated in the system at 500 K. The trend of the Brownian motion of skyrmion has been marked as black arrows. (c) Time dependence number of magnetic skyrmion under a 500 K thermal condition where (a) and (b) refer to figure panels, respectively. The number of magnetic skyrmion comes from the averaged spin configuration.

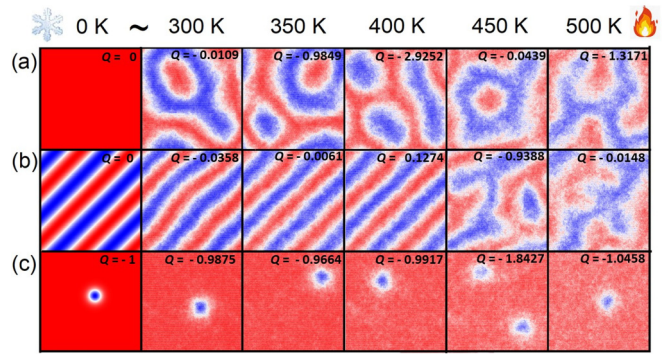


FIG. 4. The transition between the three states in the Ir/Co/Pt system (for the 10 ns simulation). (a) The phase between the Ferromagnetic phase and skyrmion+stripe domain state. (b) The transition between the stripe and skyrmion+stripe domain state. (c) The transition between the skyrmion state and skyrmion creation/annihilation state.

and shrinking of the stripe domains, which eventually leads to skyrmion nucleation in agreement with a skyrmion number of 1 and the aforementioned hybrid phase. As given in Fig. S4 in the Supplemental Material [42], the ground state of the system is the stripe domain state in absence of an external field. When a 1 T external field is applied to the system, the ground state is the skyrmion state. Simulations of the stripe domain phase with different random seeds are given in Sec. 5 of the Supplemental Material [42], showing that the final state of the system is dependent on the random thermal fluctuations. From the results in Sec. 5 of the Supplemental Material [42], the possibility of  $S_n = +1$  skyrmion creation and  $S_n = -1$  skyrmion creation in the system is the same, which suggests that these processes are equivalent in a defect-free system.

When an external field is applied to the system, the skyrmion state becomes the ground state of the system. For this state at elevated temperatures, the system goes beyond distortion of the spin texture into a region of spontaneous skyrmion creation and annihilation. Figure 3 demonstrates the creation and annihilation process for a system at  $T = 500$  K in an applied field of 1 T. The initial spin configuration for Fig. 3 is a skyrmion which is given in Fig. S3(b) in the Supplemental Material [42]. According to the spin configuration in Fig. 3, spins fluctuate in the system and spin flip events generate a spin texture which is stabilized by the DMI. To here, the DMI in the system protects the spin texture from thermal effects and the external field, and the spins are twisted around the nucleus of a magnetic skyrmion. From Fig. 3(a), a second skyrmion first generated by the thermal field grows to the same size as the original skyrmion. The size of the skyrmion is determined by the balance between exchange interaction, DMI and magnetic anisotropy, and their temperature dependence. Evidence for the annihilation of a magnetic skyrmion is given in Fig. 3(b). At this stage in the time evolution of the skyrmion state, a third skyrmion has been thermally created. Under the thermal effect, magnetic skyrmions exhibit a breathing mode, with diameters increasing and decreasing due to the thermal activation. The fluctuations lead to deformation of the skyrmion which can destroy its topological protection. As evidenced from Fig. 3(b), the size of one particular skyrmion

begins to decrease and then the skyrmion disappears from the system. From the simulation results in Fig. 3, the thermal creation and annihilation of magnetic skyrmions is clear. Furthermore, the skyrmions are easier to create by thermal fluctuations at higher temperatures and also the lifetime of skyrmions will be decreased. This is a statistical thermodynamic process and is subjected to fluctuations, but these initial results point to creation and annihilation of skyrmions at elevated temperatures. To account for the stochastic nature of thermal effects, the evolution of the system from a defined magnetic state under ten different pseudorandom number seeds is investigated and shown in Sec. 6 of the Supplemental Material [42].  $t_{\text{start}}$  is the time at which the initial magnetic configuration from which the simulations are restarted with different seeds is taken. From the simulation results presented in Fig. S6(a), when the initial state is taken at  $t_{\text{start}} = 0.30$  ns, different random fields yield a large variety of final states that range from skyrmion number 0.5 to 2.5. On the other hand, for  $t_{\text{start}} = 0.35$  ns, the system seems to evolve toward the creation of an extra skyrmion, with skyrmion No. 2. These results show that the skyrmion state, which is stabilized by DMI, can persist under thermal effects.

From the simulation results in Fig. 4(c), the skyrmion is stable and diffusive in the system due to the thermal effect. In the final state for the skyrmion at  $T = 450$  K, the image shows two skyrmions in the system, which means that at temperature greater than around 400 K, spontaneous thermal creation of skyrmions can occur. The calculated time dependence of the skyrmion number for temperatures from 450 K to 500 K is shown in Sec. 7 of the Supplemental Material [42] with a skyrmion number for the initial as 1. The observed time dependence of the skyrmion number is indicative of the creation and annihilation of skyrmions at elevated temperatures. The data show large variations over temperature because of the small system size, although a trend toward larger skyrmion numbers and more rapid creation and annihilation can be seen. Particularly, for the 500 K case, the skyrmion number is changing especially rapidly. Generation and destruction of skyrmions over time are shown in Fig. 3(a) (0.6 ns to 0.8 ns) and Fig. 3(b) (2.1 ns to 2.4 ns). The time dependence of the number of magnetic skyrmions is given in Fig. 3(c). For temperatures of  $T = 500$  K, the spontaneous creation and annihilation of skyrmions at nanosecond timescales represents a 2D skyrmion gas with a statistically varying number of particles that may be an interesting physical system to explore. The total energy of the system in a ferromagnetic state and skyrmion state at 0 K with a 1 T external field is given in Sec. 8 of the Supplemental Material [42].

The transition between different magnetic states in the Ir/Co/Pt system has been demonstrated by the simulation results and is presented in Fig. 4. For an initial ferromagnetic state, which is not the ground state of the system, the system experiences a transition toward a stripe domain state due to thermal effects. Upon further temperature increases, the system transitions to the skyrmion/stripe domain hybrid state. When the initial state of the system is the stripe domain state, with the temperature above 450 K, the stripe domain is perturbed by the thermal field and the system evolves to the skyrmion/stripe domain hybrid phase. This is similar to the case of the initial ferromagnetic state. When the simulation is set to start from a skyrmion state, this seem to remain stable up to 400 K. For temperatures greater than 450 K, thermal creation of skyrmions in the system occurs. If the temperature continues to increase around 500 K, the skyrmion may be destroyed by the thermal fluctuations and transition to a skyrmion creation/annihilation state.

#### IV. CONCLUSION

In conclusion, we have studied the magnetic phases of the Ir/Co/Pt system via an atomistic spin model. The model is based on parameters from the *ab initio* calculations and includes the full range of exchange interactions of the system. Our results show that if temperature increases, the mean skyrmion lifetime reduces and there is a larger probability of the spontaneous thermal creation/annihilation of skyrmions. Our atomistic simulations have demonstrated that the thermal skyrmion creation could occur at a temperature window much lower than the system Curie temperature. The transitions toward chiral material-systems is well explained by our model, which is important for advanced skyrmion-based spintronic devices. For example, skyrmions randomly created by thermal effects could be used as true random number generators in a computing device.

#### ACKNOWLEDGMENTS

The atomistic simulations were undertaken on the VIKING cluster, which is a high performance computing facility provided by the University of York. We are grateful for computational support from the University of York High Performance Computing service, VIKING, and the Research Computing team. The work of A.D. and L.S. was supported by the Ministry of Innovation and Technology and the National Research, Development and Innovation Office under Projects No. PD134579 and No. K131938, as well as within the Quantum Information National Laboratory of Hungary.

- 
- [1] A. Fert, V. Cros, and J. Sampaio, skyrmions on the track, *Nat. Nanotechnol.* **8**, 152 (2013).  
 [2] X. Yu, Y. Onose, N. Kanazawa, J. Park, J. Han, Y. Matsui, N. Nagaosa, and Y. Tokura, Real-space observation of a two-dimensional skyrmion crystal, *Nature (London)* **465**, 901 (2010).  
 [3] C. Pfleiderer, T. Adams, A. Bauer, W. Biberacher, B. Binz, F. Birkelbach, P. Böni, C. Franz, R. Georgii, M. Janoschek, *et al.*,

- skyrmion lattices in metallic and semiconducting B20 transition metal compounds, *J. Phys. Condes. Matter* **22**, 164207 (2010).  
 [4] S. D. Yi, S. Onoda, N. Nagaosa, and J. H. Han, skyrmions and anomalous Hall effect in a dzyaloshinskii-moriya spiral magnet, *Phys. Rev. B* **80**, 054416 (2009).  
 [5] M. N. Wilson, M. T. Birch, A. Štefančič, A. C. Twitchett-Harrison, G. Balakrishnan, T. J. Hicken, R. Fan, P. Steadman, and P. D. Hatton, *Phys. Rev. Res.* **2**, 013096 (2020).

- [6] W. Jiang, P. Upadhyaya, W. Zhang, G. Yu, M. B. Jungfleisch, F. Y. Fradin, J. E. Pearson, Y. Tserkovnyak, K. L. Wang, O. Heinonen, *et al.*, Blowing magnetic skyrmion bubbles, *Science* **349**, 283 (2015).
- [7] X. Zhang, M. Ezawa, and Y. Zhou, Magnetic skyrmion logic gates: Conversion, duplication and merging of skyrmions, *Sci. Rep.* **5**, 9400 (2015).
- [8] X. Zhang, Y. Zhou, M. Ezawa, G. Zhao, and W. Zhao, Magnetic skyrmion transistor: skyrmion motion in a voltage-gated nanotrack, *Sci. Rep.* **5**, 11369 (2015).
- [9] X. Zhang, G. Zhao, H. Fangohr, J. P. Liu, W. Xia, J. Xia, and F. Morvan, skyrmion-skyrmion and skyrmion-edge repulsions in skyrmion-based racetrack memory, *Sci. Rep.* **5**, 7643 (2015).
- [10] X. Zhang, M. Ezawa, D. Xiao, G. Zhao, Y. Liu, and Y. Zhou, All-magnetic control of skyrmions in nanowires by a spin wave, *Nanotechnology* **26**, 225701 (2015).
- [11] L. Kong and J. Zang, Dynamics of an Insulating Skyrmion Under a Temperature Gradient, *Phys. Rev. Lett.* **111**, 067203 (2013).
- [12] W. Kang, Y. Huang, C. Zheng, W. Lv, N. Lei, Y. Zhang, X. Zhang, Y. Zhou, and W. Zhao, Voltage controlled magnetic skyrmion motion for racetrack memory, *Sci. Rep.* **6**, 23164 (2016).
- [13] J. Iwasaki, M. Mochizuki, and N. Nagaosa, Current-induced skyrmion dynamics in constricted geometries, *Nat. Nanotechnol.* **8**, 742 (2013).
- [14] W. Jiang, X. Zhang, G. Yu, W. Zhang, X. Wang, M. B. Jungfleisch, J. E. Pearson, X. Cheng, O. Heinonen, K. L. Wang, *et al.*, Direct observation of the skyrmion Hall effect, *Nat. Phys.* **13**, 162 (2017).
- [15] R. Tomasello, E. Martinez, R. Zivieri, L. Torres, M. Carpentieri, and G. Finocchio, A strategy for the design of skyrmion race-track memories, *Sci. Rep.* **4**, 6784 (2014).
- [16] C. Schütte, J. Iwasaki, A. Rosch, and N. Nagaosa, Inertia, diffusion, and dynamics of a driven skyrmion, *Phys. Rev. B* **90**, 174434 (2014).
- [17] I. Limesh, K. Litzius, M. Böttcher, P. Bassirian, N. Kerber, D. Heinze, J. Zázvorka, F. Büttner, L. Caretta, M. Mann, *et al.*, Current-induced skyrmion generation through morphological thermal transitions in chiral ferromagnetic heterostructures, *Adv. Mater.* **30**, 1805461 (2018).
- [18] N. Romming, C. Hanneken, M. Menzel, J. E. Bickel, B. Wolter, K. von Bergmann, A. Kubetzka, and R. Wiesendanger, Writing and deleting single magnetic skyrmions, *Science* **341**, 636 (2013).
- [19] Z. Wang, M. Guo, H.-A. Zhou, L. Zhao, T. Xu, R. Tomasello, H. Bai, Y. Dong, S.-G. Je, W. Chao, *et al.*, Thermal generation, manipulation and thermoelectric detection of skyrmions, *Nat. Electron.* **3**, 11 (2020).
- [20] X. Yu, N. Kanazawa, Y. Onose, K. Kimoto, W. Zhang, S. Ishiwata, Y. Matsui, and Y. Tokura, Near room-temperature formation of a skyrmion crystal in thin-films of the helimagnet FeGe, *Nat. Mater.* **10**, 106 (2011).
- [21] X. Yu, N. Kanazawa, W. Zhang, T. Nagai, T. Hara, K. Kimoto, Y. Matsui, Y. Onose, and Y. Tokura, skyrmion flow near room temperature in an ultralow current density, *Nat. Commun.* **3**, 988 (2012).
- [22] T. Schulz, R. Ritz, A. Bauer, M. Halder, M. Wagner, C. Franz, C. Pfeleiderer, K. Everschor, M. Garst, and A. Rosch, Emergent electro-dynamics of skyrmions in a chiral magnet, *Nat. Phys.* **8**, 301 (2012).
- [23] H. Oike, A. Kikkawa, N. Kanazawa, Y. Taguchi, M. Kawasaki, Y. Tokura, and F. Kagawa, Interplay between topological and thermodynamic stability in a metastable magnetic skyrmion lattice, *Nat. Phys.* **12**, 62 (2016).
- [24] S.-G. Je, P. Vallobra, T. Srivastava, J.-C. Rojas-Sanchez, T. H. Pham, M. Hehn, G. Malinowski, C. Baraduc, S. Auffret, G. Gaudin, *et al.*, Creation of magnetic skyrmion bubble lattices by ultrafast laser in ultrathin films, *Nano Lett.* **18**, 7362 (2018).
- [25] R. Zivieri, R. Tomasello, O. Chubykalo-Fesenko, V. Tiberkevich, M. Carpentieri, and G. Finocchio, Configurational entropy of magnetic skyrmions as an ideal gas, *Phys. Rev. B* **99**, 174440 (2019).
- [26] J. Zazvorka, F. Jakobs, D. Heinze, N. Keil, S. Kromin, S. Jaiswal, K. Litzius, G. Jakob, P. Virnau, D. Pinna, *et al.*, Thermal skyrmion diffusion used in a reshuffler device, *Nat. Nanotechnol.* **14**, 658 (2019).
- [27] Y. Yao, X. Chen, W. Kang, Y. Zhang, and W. Zhao, Thermal Brownian motion of skyrmion for true random number generation, *IEEE Trans. Electron Devices* **67**, 2553 (2020).
- [28] D. Pinna, F. A. Araujo, J. V. Kim, V. Cros, D. Querlioz, P. Bessiere, J. Droulez, and J. Grollier, skyrmion gas manipulation for probabilistic computing, *Phys. Rev. Appl.* **9**, 064018 (2018).
- [29] F. Büttner, B. Pfau, M. Böttcher, M. Schneider, G. Mercurio, C. M. Günther, P. Helsing, C. Klose, A. Wittmann, K. Gerlinger, and L. M. Kern *et al.*, Observation of fluctuation-mediated picosecond nucleation of a topological phase, *Nat. Mater.* **20**, 30 (2021).
- [30] F. Muckel, S. von Malottki, C. Holl, B. Pestka, M. Pratzner, P. F. Bessarab, S. Heinze, and M. Morgenstern, Experimental identification of two distinct skyrmion collapse mechanisms, *Nat. Phys.* **17**, 395 (2021).
- [31] E. Simon, K. Palotás, L. Rózsa, L. Udvardi, and L. Szunyogh, Formation of magnetic skyrmions with tunable properties in PdFe bilayer deposited on Ir(111), *Phys. Rev. B* **90**, 094410 (2014).
- [32] L. Rózsa, E. Simon, K. Palotás, L. Udvardi, and L. Szunyogh, Complex magnetic phase diagram and skyrmion lifetime in an ultrathin film from atomistic simulations, *Phys. Rev. B* **93**, 024417 (2016).
- [33] R. F. Evans, W. J. Fan, P. Chureemart, T. A. Ostler, M. O. Ellis, and R. W. Chantrell, Atomistic spin model simulations of magnetic nanomaterials, *J. Phys.-Condes. Matter* **26**, 103202 (2014).
- [34] L. Szunyogh, B. Újfalussy, P. Weinberger, and J. Kollár, Self-consistent localized KKR scheme for surfaces and interfaces, *Phys. Rev. B* **49**, 2721 (1994).
- [35] R. Zeller, P. H. Dederichs, B. Újfalussy, L. Szunyogh, and P. Weinberger, Theory and convergence properties of the screened Korringa-Kohn-Rostoker method, *Phys. Rev. B* **52**, 8807 (1995).
- [36] B. L. Gyorffy, A. J. Pindor, J. Staunton, G. M. Stocks, and H. Winter, A first-principles theory of ferromagnetic phase transitions in metals, *J. Phys. F* **15**, 1337 (1985).
- [37] L. Szunyogh, L. Udvardi, J. Jackson, U. Nowak, and R. Chantrell, Atomistic spin model based on a spin-cluster

- expansion technique: Application to the IrMn<sub>3</sub>/Co interface, *Phys. Rev. B* **83**, 024401 (2011).
- [38] M. O. A. Ellis, R. F. L. Evans, T. A. Ostler, J. Barker, U. Atxitia, O. Chubykalo-Fesenko, and R. W. Chantrell, The Landau-Lifshitz equation in atomistic models, *Low Temp. Phys.* **41**, 705 (2015)
- [39] W. F. Brown Jr, Thermal fluctuations of a single-domain particle, *Phys. Rev.* **130**, 1677 (1963).
- [40] A. Lyberatos, D. V. Berkov, and R. W. Chantrell, A method for the numerical simulation of the thermal magnetization fluctuations in micromagnetics, *J. Phys.-Condes. Matter* **5**, 8911 (1993).
- [41] O. Chubykalo, R. Smirnov-Rueda, J. Gonzalez, M. Wongsam, R. W. Chantrell, and U. Nowak, Brownian dynamics approach to interacting magnetic moments, *J. Magn. Magn. Mater.* **266**, 28 (2003).
- [42] See Supplemental Material at <http://link.aps.org/supplemental/10.1103/PhysRevB.104.054420> for the temperature-dependent mean magnetization of the simulation system, parameters for the atomistic simulation, the initial spin configuration of the simulation, field-cooled simulations for the system, the stripe domain state under 450 K thermal condition with different random seed, the process of skyrmion created by thermal effect, the time dependence of the skyrmion number for temperatures from 450 K to 500 K with the external field, and the total energy of the system.
- [43] G. Yin, Y. Li, L. Kong, R. K. Lake, C. L. Chien, and J. Zang, Topological charge analysis of ultrafast single skyrmion creation, *Phys. Rev. B* **93**, 174403 (2016).
- [44] M. Hirschberger, T. Nakajima, S. Gao, L. Peng, A. Kikkawa, T. Kurumaji, M. Kriener, Y. Yamasaki, H. Sagayama, H. Nakao, *et al.*, skyrmion phase and competing magnetic orders on a breathing kagome lattice, *Nat. Commun.* **10**, 1 (2019).